



Review

# Citric Acid Derived Carbon Dots, the Challenge of Understanding the Synthesis-Structure Relationship

Junkai Ren , Luca Malfatti and Plinio Innocenzi \*

Laboratory of Materials Science and Nanotechnology (LMNT), Department of Chemistry and Pharmacy, University of Sassari, CR-INSTM, Via Vienna 2, 07100 Sassari, Italy; j.ren@studenti.uniss.it (J.R.); luca.malfatti@uniss.it (L.M.)

\* Correspondence: plinio@uniss.it

**Abstract:** Carbon dots (CDs) are highly-emissive nanoparticles obtained through fast and cheap syntheses. The understanding of CDs' luminescence, however, is still far from being comprehensive. The intense photoluminescence can have different origins: molecular mechanisms, oxidation of polyaromatic graphene-like layers, and core-shell interactions of carbonaceous nanoparticles. The citric acid (CA) is one of the most common precursors for CD preparation because of its high biocompatibility, and this review is mainly focused on CA-based CDs. The different parameters that control the synthesis, such as the temperature, the reaction time, and the choice of solvents, were critically described. Particular attention was devoted to the CDs' optical properties, such as tunable emission and quantum yields, in light of functional applications. The survey of the literature allowed correlating the preparation methods with the structures and the properties of CA-based CDs. Some basic rules to fabricate highly luminescent nanoparticles were selected by the metanalysis of the current literature in the field. In some cases, these findings can be generalized to other types of CDs prepared via liquid phase.

**Keywords:** carbon dots; citric acid; nanoparticles; photoluminescence



**Citation:** Ren, J.; Malfatti, L.; Innocenzi, P. Citric Acid Derived Carbon Dots, the Challenge of Understanding the Synthesis-Structure Relationship. *C* **2021**, *7*, 2. <https://dx.doi.org/10.3390/c7010002>

Received: 2 December 2020

Accepted: 17 December 2020

Published: 22 December 2020

**Publisher's Note:** MDPI stays neutral with regard to jurisdictional claims in published maps and institutional affiliations.



**Copyright:** © 2020 by the authors. Licensee MDPI, Basel, Switzerland. This article is an open access article distributed under the terms and conditions of the Creative Commons Attribution (CC BY) license (<https://creativecommons.org/licenses/by/4.0/>).

## 1. Introduction

Since the discovery of fluorescent carbon nanotubes fragments [1], carbon dots (CDs) have been extensively studied as an emerging generation of optoelectronic materials. The reason for such interest is due to both technological and basic science issues. The tunable photoluminescence and the high quantum yield (QY) combined with low-cost preparation [2–5] are undoubtedly attractive properties for material scientists looking for new light-emitting nanostructures. As a metal-free optical material, CDs are also environmentally friendly and represent a promising alternative to conventional metal-based semiconductors and rare elements. CDs could, therefore, potentially provide outstanding advantages in various fields, such as sensing [6,7], bioimaging [8], catalysis [9], lighting and displaying [10,11], laser [12–14], etc.

At the same time, CDs allow revolutionizing the actual perspective on the classical chemistry classifications. CDs are 0-D emissive spheroidal carbon-based nanostructures with a size smaller than 20 nm [2,5]. The CDs, in fact, stand in between organic (polymers) and inorganic materials (black carbon), macromolecules, and nanoparticle, between bottom-up (polycyclic aromatic compounds) and top-down synthesis (laser ablation of graphene, etc.). However, it is still a challenge to understand the CDs' correlation between nanostructure and bright fluorescence [15].

The number of publications about CDs has rapidly increased in recent years (see Figure 1a), reflecting the utmost simplicity in preparing the materials but also the galaxy of slightly different results that small changes in the synthesis can produce. An abundance of precursors, in fact, can be used for the preparation of CDs via bottom-up methods, ranging from simple and natural molecules up to complex and expensive compounds [16]. Among

them, citric acid (CA), a weak organic acid, is the most popular carbon precursor (see Figure 1b) because of the biocompatibility and the low cost. CA-based CDs show both photoluminescence from blue to red regions [17,18] and extremely high QYs (more than 80%) [6,19].

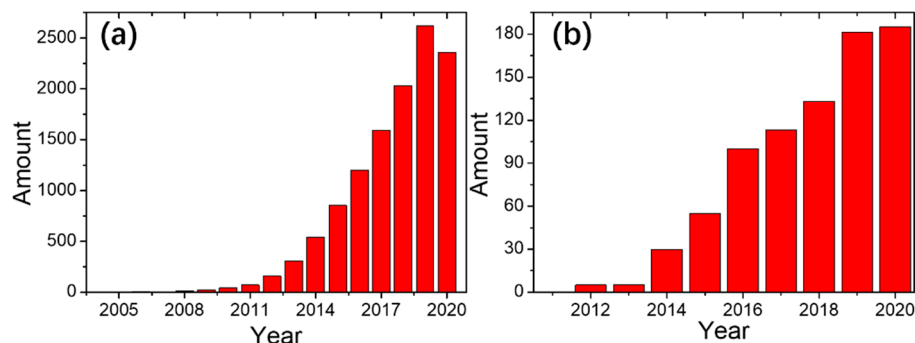


**Figure 1.** (a) Publications since 2004 retrieved by searching “carbon dots” or “carbon nanodots” or “graphene quantum dots” on Web of Science in November 2020; (b) publications since 2010 by refining the obtained result with “citric acid”.

In this review, we focused on CDs obtained via CA as the main precursor with the purpose to explore the chemistry behind the synthesis. Citric acid, among the various precursors of CDs, is undoubtedly one of the most used, as the abundant scientific literature on the topic demonstrates. Focusing on one precursor allows retrieving a series of data to model the relationships between structure and properties. CA-based CDs can be considered as one of the easiest dots to be obtained; this makes it easier to understand how and why the synthesis affects the CDs properties.

We critically reviewed most of the synthesis parameters which affect the CDs properties, including temperature, reaction time, choice of solvents, etc. Moreover, we focused on the description of CDs’ optical performances and how to improve them. Furthermore, we summarized the theoretical models of CA-based CDs by comparing the different approaches which consider the dots as large molecules or functionalized nanoparticles. Finally, we listed the new exciting applications which are foreseen in the near (bright) future of the CDs.

## 2. Towards a Retro-Engineering of the CD Structure

The striking possibility of synthesizing such bright fluorescent nanoparticles using simple protocols and cheap precursors is the reason for the broad interest in CDs. However, everything comes at a cost. The multiple carbonization reactions which drive the formation of the emitting nanoparticles are largely uncontrolled, and it appears to be difficult to disentangle such a complex network of processes occurring during the CD formation. Moreover, when hydrothermal, microwave treatment, or thermal degradation are used to synthesize CDs, the chemical reactions which lead to the formation of the carbon nanoparticles are very different from those which typically occur in organic chemistry. A careful retro-engineering process is, therefore, at the basis of real CDs nanotechnology. Bottom-up routes are effective methods to obtain high quality CDs with some organics as precursors. CDs can be synthesized from CA via hydrothermal or solvothermal methods [20–22], microwave treatments [23,24], thermal decomposition [25,26], etc. [27,28].

### 2.1. Carbonization Temperature vs. Optical Properties

It has been experimentally demonstrated that temperature is the determining factor for the carbonization of organic matters when CDs are fabricated. Many researchers have studied the influence of reaction temperature on the optical properties of CDs. We summarized some results in Figure 2, according to the published literature [6,25,29–34]. Figure 2a–e show that the QY of the prepared CDs can usually reach a maximum when the

hydrothermal temperature (HyT) is set in the range from  $\sim 150$  to  $\sim 200$  °C. The correlation between QY and HyT is the main reason why 160, 180, or 200 °C are the typical values selected for the preparation of CDs in many papers. This conclusion is not limited to hydrothermal routes but can be somewhat generalized to other approaches, such as thermal decomposition [25,33] in Figure 2f,g, and microwave treatment [34] in Figure 2h.

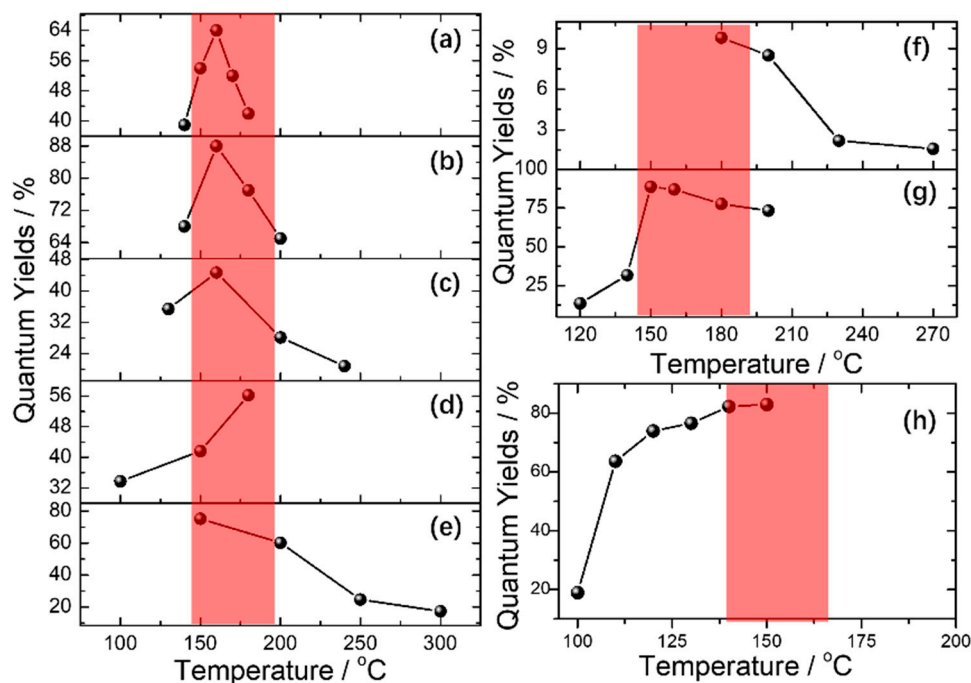


**Figure 2.** Temperature vs. quantum yields of carbon dots (CDs) synthesized from citric acid (CA) by (a–e) hydrothermal method, (f,g) thermal decomposition, and (h) microwave treatment. The data in (a–h) are organized according to the results in Ref. [29], Ref. [30], Ref. [31], Ref. [32], Ref. [6], Ref. [33] Ref. [25], and Ref. [34], respectively.

Wang et al. [35], Dhenadhayalan et al. [36], and Qu et al. [30] prepared CA-based CDs via thermal decomposition, microwave treatment (aqueous solution), and hydrothermal method, respectively, and compared the optical properties of the products. CDs show similar absorption bands, maximum emission, and QY, suggesting that CDs synthesized from the same raw materials possess similar optical features, even though different preparation ways [37–43] are carried out if the reaction temperature is kept constant (Figure 3).

It is worth considering the reason for the relationship between temperature and fluorescence intensity. A change of the morphology and the structure at a defined temperature range appears as a reasonable hypothesis. Some researchers [44–47] have studied the morphologies and the structural characterizations of CA-based CDs at different preparation temperatures. The formation of CDs is divided into different steps: dehydration, polymerization, aromatization, and carbonization. In some cases, transmission electron microscope (TEM) analyses have revealed that CDs change the structure from cross-linked polymer-like to individual nanoparticles when the temperature increases from 150 to 300 °C [48] (see Figure 4a1–d1). Furthermore, X-ray photoelectron spectroscopy (XPS) characterization has shown that the content of graphitic structure C–C/C=C in the CDs increases with the rise of temperature (see Figure 4a2–d2).

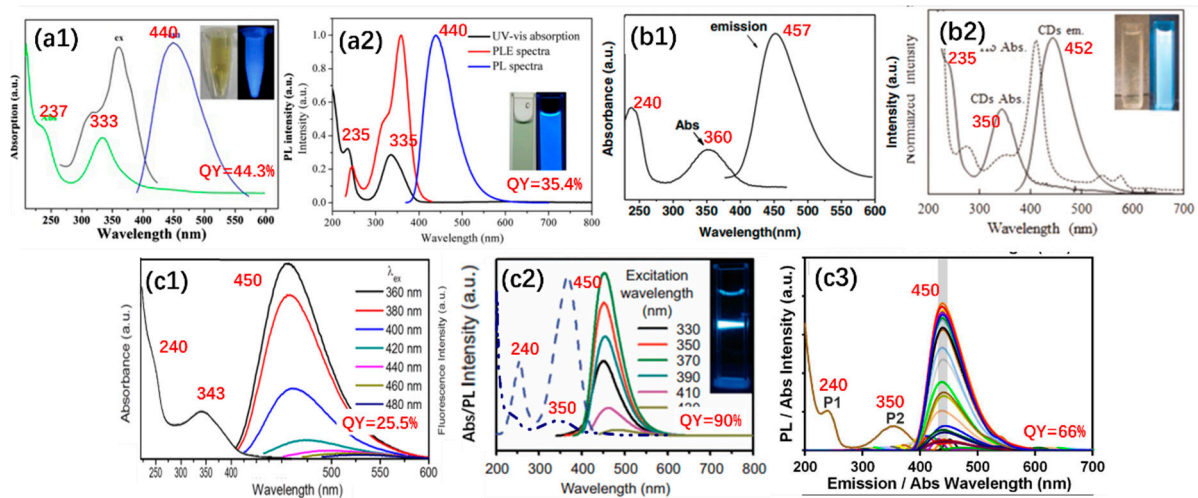


**Figure 3.** The optical properties of different CDs. CDs in (a1, Ref. [37]) and (a2, Ref. [38]) are synthesized from CA and ammonia by microwave method and hydrothermal treatment, respectively. CDs in (b1, Ref. [39]) and (b2, Ref. [40]) are synthesized from CA and ethylenediamine by microwave method and hydrothermal treatment, respectively. CDs in (c1, Ref. [41]), (c2, Ref. [42]), and (c3, Ref. [43]) are synthesized from CA and diethylenetriamine by thermal decomposition and hydrothermal treatment, respectively. Reproduced from Ref. [37–43] with permission of Copyright (2016, 2018) American Chemical Society, Copyright (2015, 2016, 2018) Elsevier, Copyright (2013) Springer, and Copyright (2015) Nature Publishing Group, respectively.

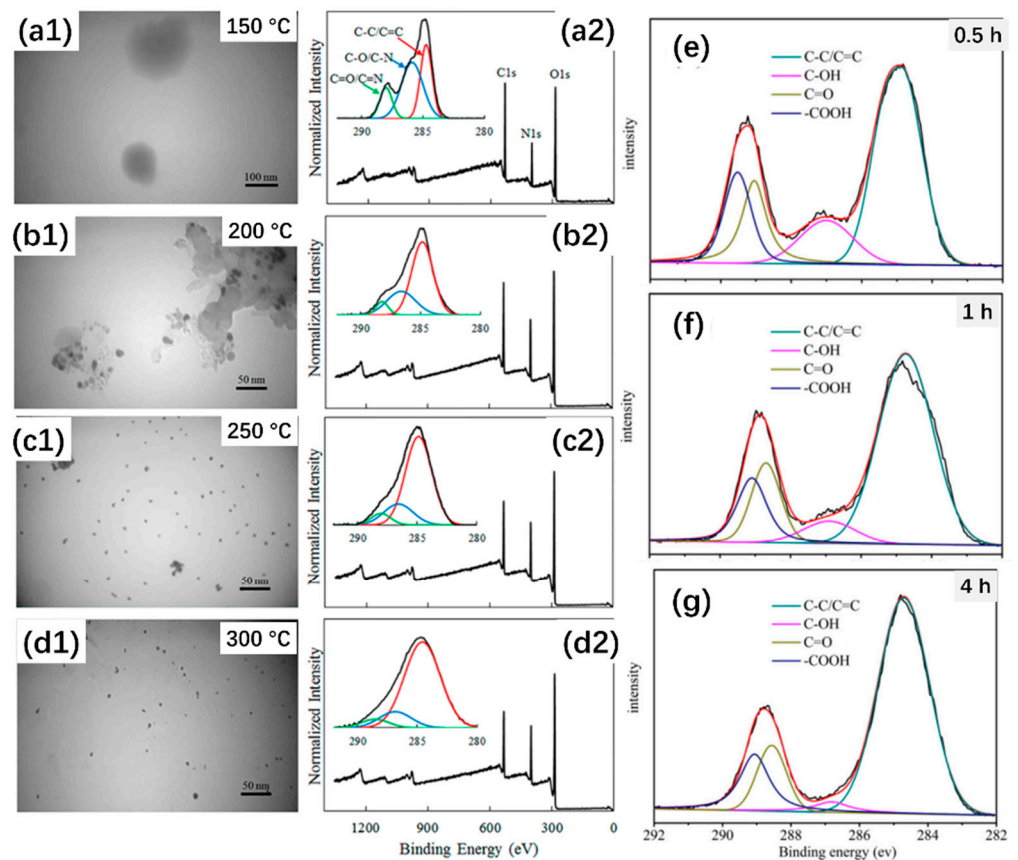


**Figure 4.** (a1–d2, Ref. [48]) TEM images and high-resolution XPS spectra of C1s of CDs prepared at different temperatures. (e–g, Ref. [49]) The high-resolution XPS spectra of C1s of CDs were prepared with different reaction times. Adopted from Ref. [48,49] with permission of Copyright (2018) American Chemical Society and Copyright (2018) Elsevier.

In a general model, the CD is made of two key parts, a carbon graphitic core and an amorphous carbon region [50–54] (see Figure 5a–e). A rise of temperature is responsible for the growth of the core and a simultaneous reduction of the amorphous region (Figure 5f) affecting the optical properties. At low temperatures, it is difficult to form a graphitic core, where, therefore, polymeric-like CDs are usually obtained. The photoluminescence of these CDs can be attributed to molecular-state emissive centers [36,48]. On the contrary, the high reaction temperatures tend to fully carbonize the functional groups of the amorphous surface. A larger size of the carbon core generally leads to a shift of photoluminescence towards larger wavelengths because of a quantum confinement effect [55,56], where the optical properties of CDs have shown a size-dependent effect. However, the carbonization of surface groups generally leads to a QY decrease. The highest QY is, therefore, achieved at an intermediate temperature range where core and shell structures coexist. It is necessary to point out that there is no clear temperature boundary to strictly control the formation of molecular-state and aromatic carbon-core domains. The coexistence of both results in multi-type CD emissions, such as size- or excitation-dependent/independent luminescence.

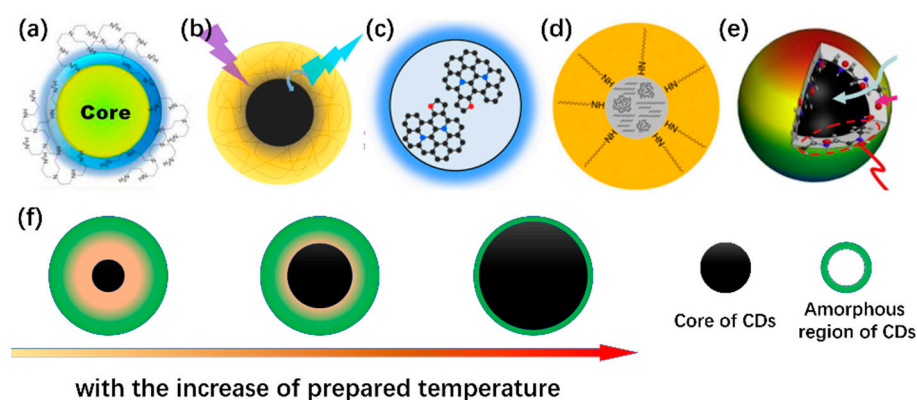


**Figure 5.** (a–e, Ref. [50–54]) Different models of CD structure diagrams. (f) Structure changes of CDs with the increase of temperature during the carbonization step. Reproduced from Ref. [50–54] with permission of Copyright (2012) American Chemical Society, Copyright (2015) Springer, Copyright (2017) Nature Publishing Group, Copyright (2014) John Wiley and Son, and Copyright (2017) Elsevier, respectively.

## 2.2. Reaction Time

The reaction time also affects the optical properties of the related CDs [18,23,25,30,57–59]. Figure 6 resumes the plots of QY vs. time measured from different CDs prepared by different groups. Although the syntheses show some differences in terms of reagents and reaction temperatures, the QY reaches a maximum in a time which depends on the reaction temperature and then decreases progressively at longer reaction times. The chemical composition vs. the reaction time shows relevant change, as shown in Figure 4e–g. In short, the rise of reaction time also leads to increased carbonization, which promotes the growth of the carbon core. This trend is similar to the changes occurring as a function of increasing temperatures so that the schematic process shown in Figure 5f is still applicable for increasing reaction times.

## 2.3. Solvothermal vs. Hydrothermal Method

The selection of solvent is critical to determine the CDs' properties. For example, blue-emitting CDs were prepared by Zhai et al. [60] through a microwave treatment using CA and ethylenediamine as the precursors and water as the solvent. The same precursors dissolved in formamide, however, allowed preparation of red-emitting CDs [61] with a ~200 nm redshift with respect to the previous protocol. Formamide plays an important role in several admixtures of reagents, enabling fine-tuning of the CDs luminescence. In a typical hydrothermal synthesis, CA and urea form mainly blue-emissive CDs, with a minor emission in the green range [62]. Hola et al. [17], however, obtained CDs with blue, green,

and red emissions by simply replacing formamide instead of water during solvothermal carbonization.

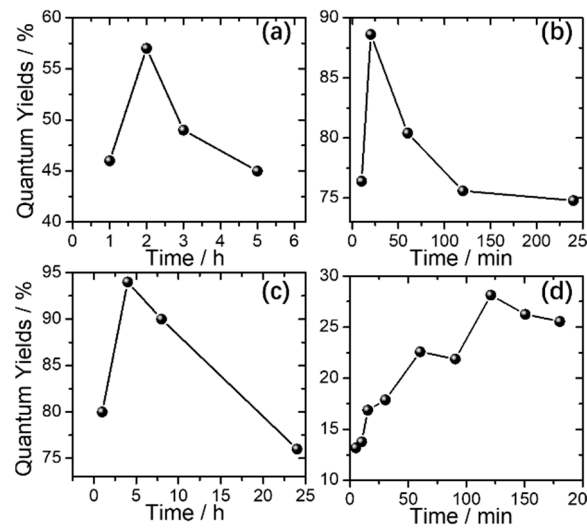


**Figure 6.** Reaction time vs. quantum yields of CDs synthesized from CA by (a,c) hydrothermal method and (b,d) thermal decomposition. The data in (a–d) are organized according to results in Ref. [57], Ref. [25], Ref. [30], and Ref. [58], respectively.

Interestingly, the reaction temperature to synthesize CA-based CDs via hydrothermal and solvothermal methods is significantly different. The example is shown in Figure 7. Although the hydrothermal temperature can be typically set in a 150–300 °C range, for instance, the maximum emission of the CDs prepared by this synthesis shows a small shift of around 20 nm [6]. On the contrary, the temperature used for the solvothermal method (dimethylformamide, DMF, as solvent) ranges from 140 to 200 °C. Still, it causes a larger shift in the CDs emission, which can exceed 80 nm [63]. It is, therefore, clear that the use of an organic solvent in the CDs synthesis promotes the carbonization process, leading to major changes in the photophysical properties of the carbon nanoparticles.

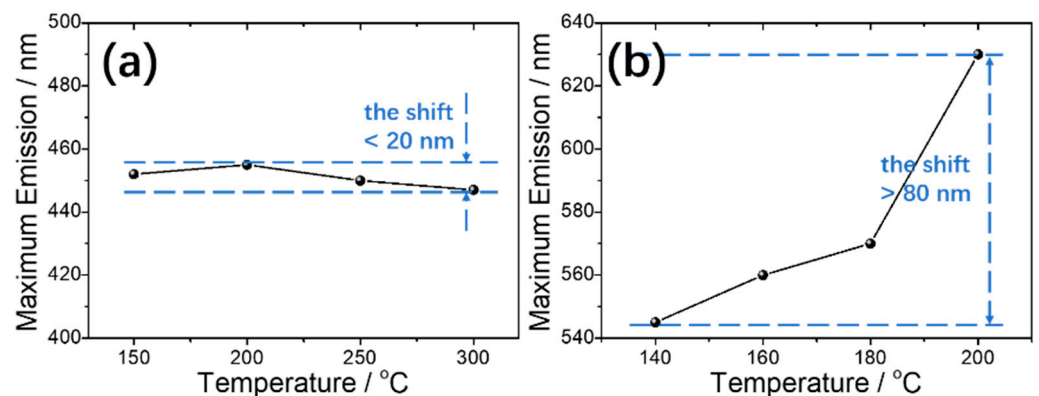


**Figure 7.** Reaction temperature vs. maximum emission of CDs synthesized from CA by (a) hydrothermal and (b) solvothermal methods. The data in (a,b) are organized according to Ref. [6] and Ref. [63], respectively.

Once prepared, the CDs must then be carefully purified to achieve a narrow emission. A lack of purification, in fact, could lead to heterogeneous results which can become very difficult to rationalize. Pan et al. [23], for instance, prepared CDs with CA dissolved in formamide and then dialyzed the products of reaction to separate the CDs with excitation-dependent multicolor emission. On the other hand, another research group [61] which

used the same materials and a similar method but a different purification process (solvent-washing) measured an excitation-independent single red photoluminescence.

Kong et al. [64] prepared blue-emitting CDs by hydrothermal treatment with CA and ethylenediamine as a precursor, coupled with dialysis purification. However, Wen et al. [65] were capable of separating the products obtained by the same synthesis through purification via column chromatography, achieving blue- and green- emissive CDs.

#### 2.4. Nitrogen Sources

There are many other parameters in the CDs preparation that have a significant impact on the properties of the products. The presence of a nitrogen source during the CD synthesis has a pivotal role in controlling the emission, however, the reactivity of the different nitrogen sources is not the same and should be carefully taken into consideration. Reckmeier et al. [66] prepared different CDs synthesized from CA using hydrothermal and ammonothermal approaches with aqueous ammonia and supercritical ammonia as the nitrogen source, respectively. They found that the two kinds of CDs are remarkably different in terms of both structure and fluorescence. On the other hand, Sharma et al. [67] obtained CDs by thermal decomposition of CA and urea under N<sub>2</sub> and air atmosphere, respectively, however, the two CDs showed similar photophysical properties.

Nitrogen-doping is also a powerful method to increase the QY of CDs photoluminescence. Table 1 compares the QYs of pure CA-based with nitrogen (N)-doped CDs. Interestingly, the N-doping provides higher QY values when specific nitrogen sources are used during the synthesis.

**Table 1.** The quantum yields of some CA-based CDs with different nitrogen (N) sources. QY: quantum yield.

Methods	Nitrogen Sources	Emission	QYs	Ref.
Hydrothermal method (200 °C, 8 h)	Phenylalanine	413 nm	65%	[20]
Microwave treatment (550 W, 7 min, aqueous solution)	-	440 nm	7.2%	[36]
Microwave treatment (700 W, 5 min, aqueous solution)	Ethylenediamine	455 nm	41.3%	[60]
Microwave treatment (700 W, 5 min, aqueous solution)	Ammonia	450 nm	44.3%	[37]
Hydrothermal method (200 °C, 5 h)	-	451 nm	7.2%	[6]
Hydrothermal method (180 °C, 4 h)	Urea	440 nm	42.2%	[62]
Hydrothermal method (200 °C, 5 h)	Ethylenediamine	470 nm	60%	[68]
Hydrothermal method (180 °C, 3 h)	Dicyandiamide	452 nm	36.5%	[69]
Hydrothermal method (200 °C, 4 h)	L-cysteine	432 nm	75%	[70]
Hydrothermal method (200 °C, 6 h)	Tri(hydroxymethyl)aminomethane	408 nm	75%	[71]
Hydrothermal method (180 °C, 4 h)	Thiourea	448 nm	73.1%	[72]

Schneider and co-workers [73] studied the influence of three different nitrogen sources on CA-based CDs: ethylenediamine, hexamethylenetetramine, and triethanolamine. As shown in Figure 8a, ethylenediamine provides the highest QY enhancement, while triethanolamine does not affect the overall fluorescent intensity. Furthermore, when doping is obtained by ethylenediamine, ethanolamine, and tris(hydroxymethyl)aminomethane as nitrogen sources, the formation of graphitic nitrogen and the enrichment of hydroxyl-groups allow forming CDs with remarkably high QY [44] (Figure 8b).

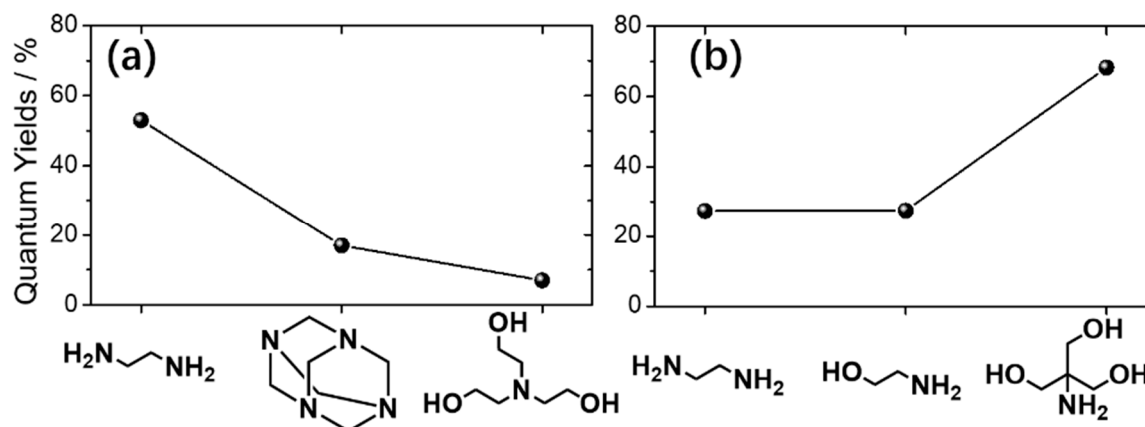


**Figure 8.** The quantum yields of CDs synthesized from CA and different nitrogen sources. The data in (a,b) are organized according to Ref. [73,74], respectively.

### 3. Optical Properties of CA-Based CDs

N-source precursors allow modulating the photophysical properties of CDs in a wide range of emissions. As shown in Table 2, the emission from CA-based CDs can be tuned from the blue to the red with remarkable QYs (>90%). The QY, however, gradually reduces when the characteristic emission is shifted towards higher wavelengths. According to the reports in Table 2, the CA-based CDs can also exhibit near-infrared photoluminescence, especially when synthesized in aprotic polar solvents, such as DMF and formamide [61,75,76].

**Table 2.** The preparation and optical properties of some CA-based CDs. DMF: dimethylformamide.

Methods	Precursors (Including CA)	Emission	QYs	Ref.
Microwave treatment (700 W, 40 s, aqueous solution)	L-cysteine	425 nm	78%	[77]
Hydrothermal method (180 °C, 8 h)	Diethylenetriamine	433 nm	98%	[78]
Hydrothermal method (200 °C, 5 h)	Ethylenediamine	445 nm	80.6%	[6]
Microwave treatment (400 W, 80 min, 150 °C, aqueous solution)	Ethylenediamine	445 nm	82.99%	[34]
Hydrothermal method (160 °C, 4 h)	Ethylenediamine	450 nm	94%	[30]
Microwave treatment (800 W, 4 min, aqueous solution)	L-cysteine, dextrin	495 nm	22%	[79]
Hydrothermal method (190 °C, 2 h)	Urea	455 nm 510 nm	29% 30%	[27]
Thermal decomposition (170 °C, 70 min)	Dicyandiamide	528 nm	73.12%	[80]
Hydrothermal method (200 °C, 4 h)	Ethylenediamine	530 nm	63.9%	[65]
Hydrothermal method (200 °C, 12 h)	Urea, ZnCl <sub>2</sub>	580 nm	51.2%	[81]
Solvothermal method (180 °C, 4 h, formamide solution)	Ethanediamine	627 nm	53%	[75]
Microwave treatment (400 W, formamide solution)	-	640 nm	22.9%	[61]
Solvothermal method (160 °C, 6 h, DMF solution)	Urea	760 nm	10%	[76]

#### 3.1. Multicolor Photoluminescence

Some specific syntheses allow preparing CA-based CDs with multicolor tunable photoluminescence. This means that minor variations of the synthesis conditions lead to different emissions. By controlling the solvothermal conditions, Miao et al. [63] prepared multiple emissive CDs as shown in Figure 9. The shift of emission from the blue to the red of the visible spectrum is related to the presence of the carboxylic groups and the increasing

graphite content in the CDs (Figure 9d). Hola and his co-workers [17] prepared multicolor emissive CDs via solvothermal treatment of CA and urea in a formamide solution. The obtained products were further purified and separated by column chromatography into four fractions showing emissions from blue to red. Herein, however, the redshift of the photoluminescence was attributed to increasing graphitic nitrogen contents, as also confirmed by time-dependent density functional theory (TD-DFT). Interestingly, all the works focused on the multicolor photoluminescence of CDs agree in considering the graphitic structure (derived from the carbonization) as a key factor to control the CDs' multicolor emission.

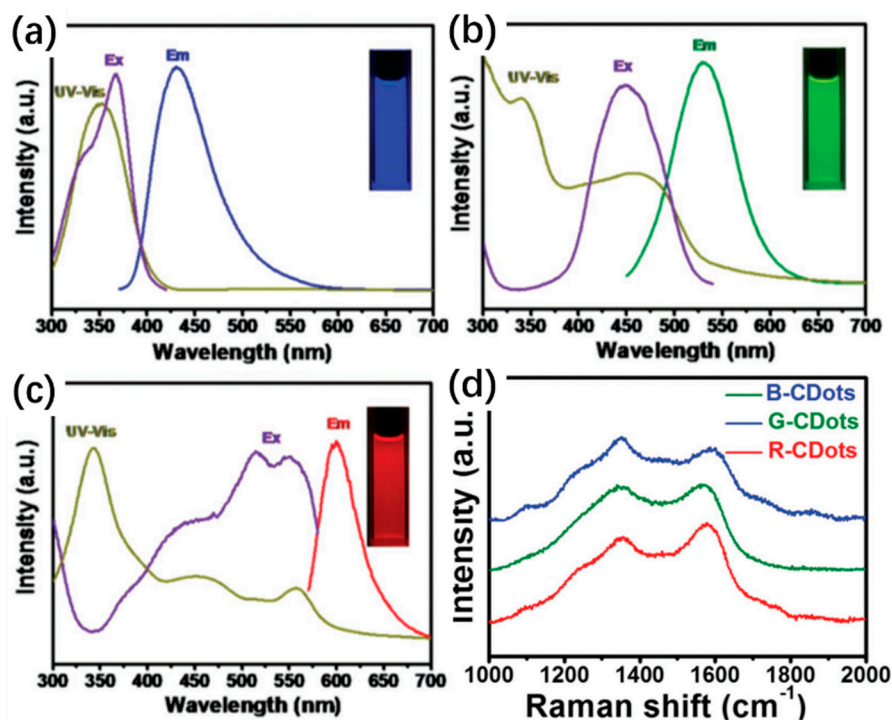


**Figure 9.** The photophysical properties of blue-, green-, and red-emitting of CDs in Ref. [63]. (a–c) UV-visible absorption, excitation, and emission, (d) Raman spectra. Reproduced from Ref. [63] with permission of Copyright (2018) John Wiley and Sons.

While the luminescence appears to be largely controlled by the degree of graphitization of the CD structure, the mechanism controlling the fluorescence is still unclear. This property seems to be affected by many other factors which induce a multicolor fluorescence. Zhu et al. [82], for example, proved that the introduction of metal ions into CA-based CDs structure prepared via magnetic hyperthermia approach leads to a multicolor-fluorescence over a wide range of the visible spectrum. Moreover, some CDs exhibit a long fluorescence lifetime, such as long afterglow performance. CDs fabricated via hydrothermal treatment of CA, acrylamide, and urea exhibit room-temperature phosphorescence with a long lifetime reaching up to 459 ms [83]. Boron is also an important doping agent in the development of CDs featuring ultralong lifetime room temperature phosphorescence. Boron-doped CDs exhibit bright yellow-green afterglow with a remarkable QY of 23.5% and a lifetime of 1.17 s [84].

### 3.2. Surface Modifications

Surface modification is, in general, an effective strategy to enhance CDs' optical performances. Usually, the CDs obtained by pyrolysis of CA show a weak fluorescence with a short lifetime. In our previous work [59], it was found that the surface functionalization with 3-aminopropyltriethoxysilane (APTES) reduces the CDs fluorescence quenching due to the formation of a passivation layer. The 3-glycidyloxypropyltrimethoxysilane (GPTMS)

is also a possible alternative to modify the surface via an epoxy-amine reaction [22]. In addition to the native luminescence at 430 nm, the GPTMS-grafted CDs show a new emission at 490 nm due to the polyethylene oxide species.

Liu et al. [85] prepared highly emissive solid-state CDs via one-step hydrothermal method with CA as the carbon source and branched poly(ethylenimine) (b-PEI) as the surface passivation agent. The introduction of b-PEI chains can prevent the collisions of CD emissive centers, which further avoids the aggregation-induced quenching.

### 3.3. External Variables Controlling the Emission

The optical response of phosphors, including CDs, usually are temperature dependent. Kalytchuk et al. [86] prepared nitrogen/sulfur-co-doped CDs by hydrothermal treatment of CA and L-cysteine, which show temperature-dependent absorption, steady-state and transient photoluminescence, and lifetime. The sensitivity to external temperature enables the use of CDs as nano-thermometers featuring good sensitivity [87].

When CDs are used in solution, pH is also a pivotal parameter capable of tuning the emission. CDs made of CA and polyethylenimine (PEI) or 2,3-diaminopyridine (DAP) have shown a reduction of the QYs from  $\approx 40\text{--}50\%$  to less than 9% when dissolved in an aqueous solution of  $\text{pH} \approx 1$  and to 21% when the pH has been increased to 12 [88]. The peculiar behavior of some CD's fluorophores formed in situ during CDs carbonization, such as citrazinic acid, has also been recently studied at extreme pH conditions [89,90]. The same fluorophores dissolved in solution have also proved to drastically change their optical properties as a function of the concentration undergoing a transition from monomer to dimer [91]. Concentration-dependent emission is another feature of CDs, which is usually compared with aggregation-induced emission. Wang et al. [37] synthesized a type of concentration-dependent fluorescent CD by microwave treatment of CA and ammonia. The photoluminescence shows a remarkable red-shift when the CDs' concentration increases from 0.78 to 10.42  $\text{mg mL}^{-1}$  in an aqueous solution.

The abundant surface groups, e.g.,  $-\text{COOH}$ ,  $-\text{NH}_2$ , and  $-\text{OH}$ , contribute to the high solubility of CDs in water. Red-emitting CDs, however, are not prepared by hydrothermal treatment but rather via solvothermal routes employing DMF, ethanol, etc., as solvents [18,63]. Red emitting CDs typically have a low solubility in water with lower QYs [61,75,76]. For example, the 53% QY of red CDs in EtOH drops to 24% when dispersed in water [75].

## 4. Optical Applications

The excellent optical properties make CDs a promising material to be used in many potential applications, as resumed in Figure 10. The strong absorption endowed by the CDs could be efficiently applied to ultraviolet shielding devices [92]. It is also widely recognized that CDs boost the photocatalytic reactions. CD-based photocatalysts also work well in the near-infrared region where up-conversion is observed [93,94]. CDs-based devices are expected to replace toxic compounds or rare elements in monitors and fluorescent bulbs even if, at the moment, they lack the efficiency requested in the red region. The state of the art for CA-based CDs is multicolor emission with QYs exceeding 50% in the red [65,75,77].

The surface functionalization has already proved to further enhance the CD's optical properties. Organosilane-linked CDs [95,96], for instance, show both down and up-conversion photoluminescence and exhibit significant multi-photon absorption at room temperature [97]. Although multiphoton excited fluorescence is an emerging research topic, however, it is clear that specifically designed CDs could provide dramatic advances in cutting-edge optical applications such as infrared light detectors, microcavity lasers, etc.

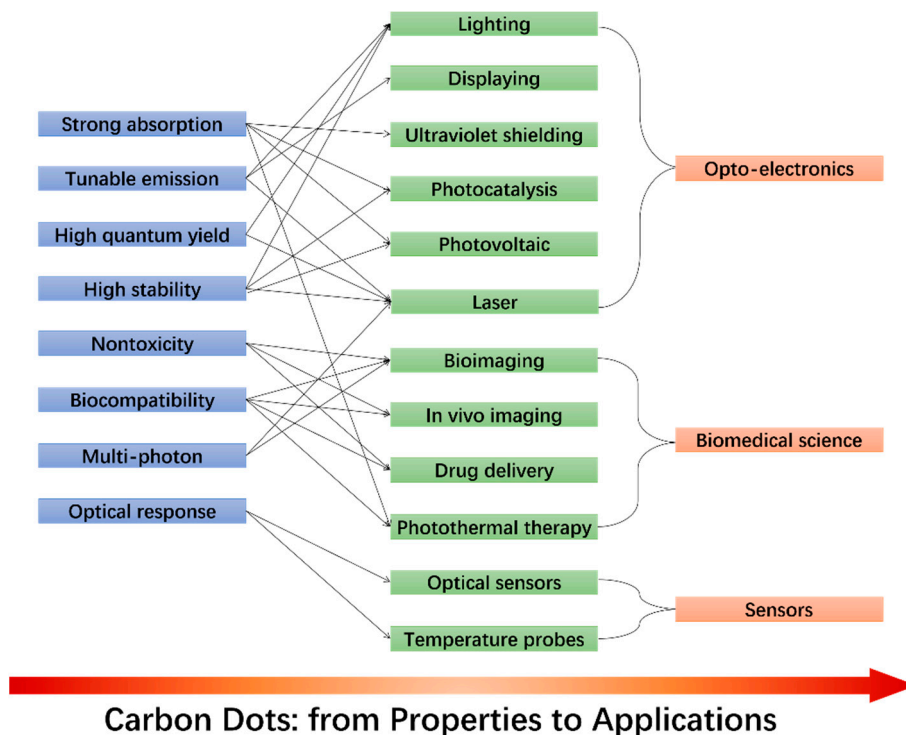


Figure 10. CDs' optical properties and potential applications.

CDs are sensitive to environment changes, such as pH, ions strength, and temperature, which set the conditions for CDs-based optical sensors. For example, CDs with hydroxyl and carboxyl groups on their surface have shown to work well as pH sensors [98]. Currently, CDs have been extensively used to detect iron (III) due to a strong coordination interaction between  $\text{Fe}^{3+}$  and the phenolic groups of CDs [6]. Finally, the nontoxicity and the biocompatibility make CDs ideal nanomaterials to develop innovative bioimaging techniques [43,99], biosensors [100], drug-delivery carriers [101], and nano-based antioxidant formulations [102,103].

In the future, new and effective technologies are required for low-cost production of high-quantity CDs.

## 5. Summary and Outlook

The general trends retrieved from the studies on CA-based CDs can be easily extended to a larger variety of CDs. CDs prepared from folic acid, for instance, show a variable QY which is related to the reaction temperature and has a maximum of around 240 °C [104]. This finding agrees with the correlation between QY and reaction temperature of CA-based CDs.

The choice of the solvent in a solvothermal synthesis is also generally affecting the optical properties and the QY of the products, even for CDs not based on CA. Paraphenylenediamine-based CDs synthesized in water, for instance, show two characteristic emissions, one at 600 nm (red) and a second one at 400 nm (blue). If the reaction solvent is replaced with ethanol, DMF, cyclohexane, or toluene, the red emission increases in intensity, while the blue one decreases [105].

Finally, the increase of graphitic carbon domains generally causes a redshift of photoluminescence in the CDs, although the same effect can be also attributed to other parameters (such as the graphitic nitrogen), especially for CDs not based on CA [106].

Although there is large variability in chemical composition and structure of the different CDs, the large number of works published thus far allows identifying some general trends and common phenomena in the preparation and the optical performances of the CDs.

The carbonization temperature is a key factor for controlling the growth of the carbon core and the density of surface groups in the CDs systems. A carbon core is usually obtained at high temperature, while the surface groups reduce as a function of the temperatures. An intermediate temperature (150–200 °C for CA-based CDs), therefore, should be considered to maximize the QY.

Reaction time plays a role similar to the reaction temperature in the CDs' synthesis. Extending the carbonization for longer times enhances the degree of carbonization and reduces the functional groups on the surface. In the quest of CDs with high QYs, it is, therefore, of paramount importance to optimize the reaction time to achieve a compromise between the core formation and the chemical composition of the surface. When a solvothermal approach is used, the choice of the solvent affects the CDs fluorescence. Generally speaking, the solvents can also serve as nitrogen sources towards doping of the CDs' structure.

CA-based CDs show multicolor fluorescence. However, the maximum of the emission is shifted towards longer wavelengths when organic, apolar, and N-containing solvents are used instead of water during the solvothermal synthesis. The nitrogen-doping dramatically contributes to enhancing the QY. This effect, however, depends on the chemical composition of the reagents used for doping. It has been found that, in general, primary amines allows increasing the QY more than secondary and tertiary amines  $\text{NH}_2 > \text{-NH-} > \text{N}\equiv$ .

Although the machinery of CD fluorescence is still mostly unexplored, it seems that both amorphous and graphitic carbon atoms could contribute to this effect. The size of the carbon core also influences the emission due to the quantum confinement effect by red shifting the fluorescence redshift.

Concerning the technological advancements, although the CDs show a set of promising features, full optimization of the photophysical properties is required to promote the development of innovative functional devices.

**Author Contributions:** The original draft was written by J.R. and L.M., supervision was performed by L.M. and P.I., the final version was edited by all authors. All authors have read and agreed to the published version of the manuscript.

**Funding:** This research was funded by Italian Ministry of University and Research (MUR) through project PRIN2017 "CANDL2", grant number 2017W75RAE.

**Data Availability Statement:** All data generated or analyzed during this study are included in this article.

**Conflicts of Interest:** The authors declare no conflict of interest.

## References

1. Xu, X.; Ray, R.; Gu, Y.; Ploehn, H.J.; Gearheart, L.; Raker, K.; Scrivens, W.A. Electrophoretic analysis and purification of fluorescent single-walled carbon nanotube fragments. *J. Am. Chem. Soc.* **2004**, *126*, 12736. [[CrossRef](#)]
2. Zhu, S.; Song, Y.; Zhao, X.; Shao, J.; Zhang, J.; Yang, B. The photoluminescence mechanism in carbon dots (graphene quantum dots, carbon nanodots, and polymer dots): Current state and future perspective. *Nano Res.* **2015**, *8*, 355. [[CrossRef](#)]
3. Cao, L.; Wang, X.; Meziani, M.J.; Lu, F.; Wang, H.; Luo, P.G.; Lin, Y.; Harruff, B.A.; Veca, L.M.; Murray, D. Carbon dots for multiphoton bioimaging. *J. Am. Chem. Soc.* **2007**, *129*, 11318. [[CrossRef](#)]
4. Zheng, X.T.; Ananthanarayanan, A.; Luo, K.Q.; Chen, P. Glowing graphene quantum dots and carbon dots: Properties, syntheses, and biological applications. *Small* **2015**, *11*, 1620. [[CrossRef](#)] [[PubMed](#)]
5. Malfatti, L.; Innocenzi, P. Sol-gel chemistry for carbon dots. *Chem. Rec.* **2018**, *18*, 1192. [[CrossRef](#)] [[PubMed](#)]
6. Zhu, S.; Meng, Q.; Wang, L.; Zhang, J.; Song, Y.; Jin, H.; Zhang, K.; Sun, H.; Wang, H.; Yang, B. Highly photoluminescent carbon dots for multicolor patterning, sensors, and bioimaging. *Angew. Chem. Int. Ed.* **2013**, *52*, 3953. [[CrossRef](#)] [[PubMed](#)]
7. Yang, D.; Ren, J.; Li, J.; Wang, Q.; Wang, Q.; Xie, Z.; Qu, X. Construction of bi-layer biluminophore fast-responding pressure sensitive coating for non-contact unsteady aerodynamic testing. *Polym. Test.* **2019**, *77*, 105922. [[CrossRef](#)]
8. Luo, P.G.; Sahu, S.; Yang, S.; Sonkar, S.K.; Wang, J.; Wang, H.; LeCroy, G.E.; Cao, L.; Sun, Y. Carbon "quantum" dots for optical bioimaging. *J. Mater. Chem.* **2013**, *1*, 2116. [[CrossRef](#)]
9. Hutton, G.A.; Martindale, B.C.; Reisner, E. Carbon dots as photosensitisers for solar-driven catalysis. *Chem. Soc. Rev.* **2017**, *46*, 6111. [[CrossRef](#)]
10. Wang, F.; Chen, Y.; Liu, C.; Ma, D. White light-emitting devices based on carbon dots' electroluminescence. *Chem. Commun.* **2011**, *47*, 3502. [[CrossRef](#)]

11. Ren, J.; Sun, J.; Sun, X.; Song, R.; Xie, Z.; Zhou, S. Precisely controlled up/down-conversion liquid and solid state photoluminescence of carbon dots. *Adv. Opt. Mater.* **2018**, *6*, 1800115. [[CrossRef](#)]
12. Zhang, W.; Zhu, H.; Yu, S.; Yang, H. Observation of lasing emission from carbon nanodots in organic solvents. *Adv. Mater.* **2012**, *24*, 2263. [[CrossRef](#)] [[PubMed](#)]
13. Ren, J.; Sun, X.; Wang, Y.; Song, R.; Xie, Z.; Zhou, S.; Chen, P. Controllable photoluminescent and nonlinear optical properties of polymerizable carbon dots and their arbitrary copolymerized gel glasses. *Adv. Opt. Mater.* **2018**, *6*, 1701273. [[CrossRef](#)]
14. Han, Z.; Ni, Y.; Ren, J.; Zhang, W.; Wang, Y.; Xie, Z.; Zhou, S.; Yu, S.F. Highly efficient and ultra-narrow bandwidth orange emissive carbon dots for microcavity lasers. *Nanoscale* **2019**, *11*, 11577. [[CrossRef](#)]
15. Ren, J.; Stagi, L.; Innocenzi, P. Fluorescent carbon dots in solid-state: From nanostructures to functional devices. *Prog. Solid State Chem.* **2020**, 100295. [[CrossRef](#)]
16. Semeniuk, M.; Yi, Z.; Poursorkhabi, V.; Tjong, J.; Jaffer, S.; Lu, Z.-H.; Sain, M. Future perspectives and review on organic carbon dots in electronic applications. *ACS Nano* **2019**, *13*, 6224. [[CrossRef](#)]
17. Hola, K.; Sudolska, M.; Kalytchuk, S.; Nachtigallova, D.; Rogach, A.L.; Otyepka, M.; Zboril, R. Graphitic nitrogen triggers red fluorescence in carbon dots. *ACS Nano* **2017**, *11*, 12402. [[CrossRef](#)]
18. Yuan, F.; Wang, Z.; Li, X.; Li, Y.; Tan, Z.; Fan, L.; Yang, S. Bright multicolor bandgap fluorescent carbon quantum dots for electroluminescent light-emitting diodes. *Adv. Mater.* **2017**, *29*, 1604436. [[CrossRef](#)]
19. Xie, Z.; Wang, F.; Liu, C. Organic-inorganic hybrid functional carbon dot gel glasses. *Adv. Mater.* **2012**, *24*, 1716. [[CrossRef](#)]
20. Chahal, S.; Yousefi, N.; Tufenkji, N. Green synthesis of high quantum yield carbon dots from phenylalanine and citric acid: Role of stoichiometry and nitrogen doping. *ACS Sustain. Chem. Eng.* **2020**, *8*, 5566–5575. [[CrossRef](#)]
21. Qu, S.; Zhou, D.; Li, D.; Ji, W.; Jing, P.; Han, D.; Liu, L.; Zeng, H.; Shen, D. Toward efficient orange emissive carbon nanodots through conjugated sp<sup>2</sup>-domain controlling and surface charges engineering. *Adv. Mater.* **2016**, *28*, 3516. [[CrossRef](#)] [[PubMed](#)]
22. Suzuki, K.; Malfatti, L.; Takahashi, M.; Carboni, D.; Messina, F.; Tokudome, Y.; Takemoto, M.; Innocenzi, P. Design of carbon dots photoluminescence through organo-functional silane grafting for solid-state emitting devices. *Sci. Rep.* **2017**, *7*, 5469. [[CrossRef](#)] [[PubMed](#)]
23. Pan, L.; Sun, S.; Zhang, A.; Jiang, K.; Zhang, L.; Dong, C.; Huang, Q.; Wu, A.; Lin, H. Truly fluorescent excitation-dependent carbon dots and their applications in multicolor cellular imaging and multidimensional sensing. *Adv. Mater.* **2015**, *27*, 7782. [[CrossRef](#)] [[PubMed](#)]
24. Carbonaro, C.M.; Chiriu, D.; Stagi, L.; Casula, M.F.; Thakkar, S.V.; Malfatti, L.; Suzuki, K.; Ricci, P.C.; Corpino, R. Carbon dots in water and mesoporous matrix: Chasing the origin of their photoluminescence. *J. Phys. Chem.* **2018**, *122*, 25638. [[CrossRef](#)]
25. Yin, C.; Fan, Y.; Yang, X.; Zhou, X. Highly efficient synthesis of N-doped carbon dots with excellent stability through pyrolysis method. *J. Mater. Sci.* **2019**, *54*, 9372. [[CrossRef](#)]
26. Kasprzyk, W.; Bednarz, S.; Żmudzki, P.; Galica, M.; Bogdał, D. Novel efficient fluorophores synthesized from citric acid. *RSC Adv.* **2015**, *5*, 34795. [[CrossRef](#)]
27. Mura, S.; Ludmerczki, R.; Stagi, L.; Garroni, S.; Carbonaro, C.M.; Ricci, P.C.; Casula, M.F.; Malfatti, L.; Innocenzi, P. Integrating sol-gel and carbon dots chemistry for the fabrication of fluorescent hybrid organic-inorganic films. *Sci. Rep.* **2020**, *10*, 4770. [[CrossRef](#)]
28. Das, A.; Gude, V.; Roy, D.; Chatterjee, T.; De, C.K.; Mandal, P.K. On the molecular origin of photoluminescence of nonblinking carbon dot. *J. Phys. Chem.* **2017**, *121*, 9634. [[CrossRef](#)]
29. Liao, S.; Zhao, X.; Zhu, F.; Chen, M.; Wu, Z.; Yang, H.; Chen, X. Novel S, N-doped carbon quantum dot-based “off-on” fluorescent sensor for silver ion and cysteine. *Talanta* **2018**, *180*, 300. [[CrossRef](#)]
30. Qu, D.; Zheng, M.; Zhang, L.; Zhao, H.; Xie, Z.; Jing, X.; Haddad, R.E.; Fan, H.; Sun, Z. Formation mechanism and optimization of highly luminescent N-doped graphene quantum dots. *Sci. Rep.* **2014**, *4*, 5294. [[CrossRef](#)]
31. Li, X.; Zhang, S.; Kulinich, S.A.; Liu, Y.; Zeng, H. Engineering surface states of carbon dots to achieve controllable luminescence for solid-luminescent composites and sensitive Be<sup>2+</sup> detection. *Sci. Rep.* **2014**, *4*, 4976. [[CrossRef](#)]
32. Kundu, A.; Lee, J.; Park, B.; Ray, C.; Sankar, K.V.; Kim, W.S.; Lee, S.H.; Cho, I.-J.; Jun, S.C. Facile approach to synthesize highly fluorescent multicolor emissive carbon dots via surface functionalization for cellular imaging. *J. Colloid Interface Sci.* **2018**, *513*, 505. [[CrossRef](#)] [[PubMed](#)]
33. Wang, S.; Chen, Z.; Cole, I.; Li, Q. Structural evolution of graphene quantum dots during thermal decomposition of citric acid and the corresponding photoluminescence. *Carbon* **2015**, *82*, 304. [[CrossRef](#)]
34. Xiao, Q.; Liang, Y.; Zhu, F.; Lu, S.; Huang, S. Microwave-assisted one-pot synthesis of highly luminescent N-doped carbon dots for cellular imaging and multi-ion probing. *Microchim. Acta* **2017**, *184*, 2429. [[CrossRef](#)]
35. Wang, J.; Wei, J.; Su, S.; Qiu, J. Novel fluorescence resonance energy transfer optical sensors for vitamin B<sub>12</sub> detection using thermally reduced carbon dots. *New J. Chem.* **2015**, *39*, 501. [[CrossRef](#)]
36. Dhenadhayalan, N.; Lin, K.C.; Suresh, R.; Ramamurthy, P. Unravelling the multiple emissive states in citric-acid-derived carbon dots. *J. Phys. Chem.* **2016**, *120*, 1252. [[CrossRef](#)]
37. Wang, C.; Hu, T.; Wen, Z.; Zhou, J.; Wang, X.; Wu, Q.; Wang, C. Concentration-dependent color tunability of nitrogen-doped carbon dots and their application for iron (III) detection and multicolor bioimaging. *J. Colloid Interface Sci.* **2018**, *521*, 33. [[CrossRef](#)]
38. Zhang, Y.; Cui, P.; Zhang, F.; Feng, X.; Wang, Y.; Yang, Y.; Liu, X. Fluorescent probes for “off-on” highly sensitive detection of Hg<sup>2+</sup> and L-cysteine based on nitrogen-doped carbon dots. *Talanta* **2016**, *152*, 288. [[CrossRef](#)]

39. Du, F.; Zeng, F.; Ming, Y.; Wu, S. Carbon dots-based fluorescent probes for sensitive and selective detection of iodide. *Microchim. Acta* **2013**, *180*, 453. [[CrossRef](#)]
40. Barati, A.; Shamsipur, M.; Abdollahi, H. Hemoglobin detection using carbon dots as a fluorescence probe. *Biosens. Bioelectron.* **2015**, *71*, 470. [[CrossRef](#)]
41. Feng, T.; Ai, X.; An, G.; Yang, P.; Zhao, Y. Charge-convertible carbon dots for imaging-guided drug delivery with enhanced in vivo cancer therapeutic efficiency. *ACS Nano* **2016**, *10*, 4410. [[CrossRef](#)] [[PubMed](#)]
42. Qu, D.; Zheng, M.; Li, J.; Xie, Z.; Sun, Z. Tailoring color emissions from N-doped graphene quantum dots for bioimaging applications. *Light Sci. Appl.* **2015**, *4*, 364. [[CrossRef](#)]
43. Wang, J.; Zhang, P.; Huang, C.; Liu, G.; Leung, K.C.F.; Wang, Y.X.N.J. High performance photoluminescent carbon dots for in vitro and in vivo bioimaging: Effect of nitrogen doping ratios. *Langmuir* **2015**, *31*, 8063. [[CrossRef](#)] [[PubMed](#)]
44. Xiong, Y.; Schneider, J.; Reckmeier, C.J.; Huang, H.; Kasák, P.; Rogach, A.L. Carbonization conditions influence the emission characteristics and the stability against photobleaching of nitrogen doped carbon dots. *Nanoscale* **2017**, *9*, 11730. [[CrossRef](#)] [[PubMed](#)]
45. Ogi, T.; Aishima, K.; Permatasari, F.A.; Iskandar, F.; Tanabe, E.; Okuyama, K. Kinetics of nitrogen-doped carbon dot formation via hydrothermal synthesis. *New J. Chem.* **2016**, *40*, 5555. [[CrossRef](#)]
46. Dong, Y.; Shao, J.; Chen, C.; Li, H.; Wang, R.; Chi, Y.; Lin, X.; Chen, G. Blue luminescent graphene quantum dots and graphene oxide prepared by tuning the carbonization degree of citric acid. *Carbon* **2012**, *50*, 4738. [[CrossRef](#)]
47. Zhou, Y.; Desserre, A.; Sharma, S.K.; Li, S.; Marksberry, M.H.; Chusuei, C.C.; Blackwelder, P.L.; Leblanc, R.M. Gel-like carbon dots: Characterization and their potential applications. *ChemPhysChem* **2017**, *18*, 890. [[CrossRef](#)]
48. Shamsipur, M.; Barati, A.; Taherpour, A.A.; Jamshidi, M. Resolving the multiple emission centers in carbon dots: From fluorophore molecular states to aromatic domain states and carbon-core states. *J. Phys. Chem. Lett.* **2018**, *9*, 4189. [[CrossRef](#)]
49. Shang, W.; Cai, T.; Zhang, Y.; Liu, D.; Liu, S. Facile one pot pyrolysis synthesis of carbon quantum dots and graphene oxide nanomaterials: All carbon hybrids as eco-environmental lubricants for low friction and remarkable wear-resistance. *Tribol. Int.* **2018**, *118*, 373. [[CrossRef](#)]
50. Dong, Y.; Wang, R.; Li, G.; Chen, C.; Chi, Y.; Chen, G. Polyamine-functionalized carbon quantum dots as fluorescent probes for selective and sensitive detection of copper ions. *Anal. Chem.* **2012**, *84*, 6220. [[CrossRef](#)]
51. Deng, L.; Wang, X.; Kuang, Y.; Wang, C.; Luo, L.; Wang, F.; Sun, X. Development of hydrophilicity gradient ultracentrifugation method for photoluminescence investigation of separated non-sedimental carbon dots. *Nano Res.* **2015**, *8*, 2810. [[CrossRef](#)]
52. Bhattacharyya, S.; Ehrat, F.; Urban, P.; Teves, R.; Wyrwich, R.; Döblinger, M.; Feldmann, J.; Urban, A.S.; Stolarczyk, J.K. Effect of nitrogen atom positioning on the trade-off between emissive and photocatalytic properties of carbon dots. *Nat. Commun.* **2017**, *8*, 1401. [[CrossRef](#)] [[PubMed](#)]
53. Kwon, W.; Lee, G.; Do, S.; Joo, T.; Rhee, S.W. Size-controlled soft-template synthesis of carbon nanodots toward versatile photoactive materials. *Small* **2014**, *10*, 506. [[CrossRef](#)] [[PubMed](#)]
54. Hou, X.; Hu, Y.; Wang, P.; Yang, L.; Al Awak, M.M.; Tang, Y.; Twara, F.K.; Qian, H.; Sun, Y. Modified facile synthesis for quantitatively fluorescent carbon dots. *Carbon* **2017**, *122*, 389. [[CrossRef](#)] [[PubMed](#)]
55. Zhu, J.; Bai, X.; Chen, X.; Shao, H.; Zhai, Y.; Pan, G.; Zhang, H.; Ushakova, E.V.; Zhang, Y.; Song, H. Spectrally tunable solid state fluorescence and room-temperature phosphorescence of carbon dots synthesized via seeded growth method. *Adv. Opt. Mater.* **2019**, *7*, 1801599. [[CrossRef](#)]
56. Wang, B.; Yu, J.; Sui, L.; Zhu, S.; Tang, Z.; Yang, B.; Lu, S. Rational design of multi-color-emissive carbon dots in a single reaction system by hydrothermal. *Adv. Sci.* **2020**, 2001453. [[CrossRef](#)]
57. Gao, F.; Ma, S.; Li, J.; Dai, K.; Xiao, X.; Zhao, D.; Gong, W. Rational design of high quality citric acid-derived carbon dots by selecting efficient chemical structure motifs. *Carbon* **2017**, *112*, 131. [[CrossRef](#)]
58. Wang, F.; Pang, S.; Wang, L.; Li, Q.; Kreiter, M.; Liu, C.Y. One-step synthesis of highly luminescent carbon dots in noncoordinating solvents. *Chem. Mater.* **2010**, *22*, 4528. [[CrossRef](#)]
59. Ludmerczki, R.; Mura, S.; Carbonaro, C.M.; Mandity, I.M.; Carraro, M.; Senes, N.; Garroni, S.; Granozzi, G.; Calvillo, L.; Marras, S. Carbon dots from citric acid and its intermediates formed by thermal decomposition. *Chem. Eur. J.* **2019**, *25*, 11963. [[CrossRef](#)]
60. Zhai, Y.; Zhu, Z.; Zhu, C.; Ren, J.; Wang, E.; Dong, S. Multifunctional water-soluble luminescent carbon dots for imaging and Hg<sup>2+</sup> sensing. *J. Mater. Chem.* **2014**, *2*, 6995. [[CrossRef](#)]
61. Sun, S.; Zhang, L.; Jiang, K.; Wu, A.; Lin, H. Toward high-efficient red emissive carbon dots: Facile preparation, unique properties, and applications as multifunctional theranostic agents. *Chem. Mater.* **2016**, *28*, 8659. [[CrossRef](#)]
62. Zhang, Y.; He, Y.; Cui, P.; Feng, X.; Chen, L.; Yang, Y.; Liu, X. Water-soluble, nitrogen-doped fluorescent carbon dots for highly sensitive and selective detection of Hg<sup>2+</sup> in aqueous solution. *RSC Adv.* **2015**, *5*, 40393. [[CrossRef](#)]
63. Miao, X.; Qu, D.; Yang, D.; Nie, B.; Zhao, Y.; Fan, H.; Sun, Z. Synthesis of carbon dots with multiple color emission by controlled graphitization and surface functionalization. *Adv. Mater.* **2018**, *30*, 1704740. [[CrossRef](#)] [[PubMed](#)]
64. Kong, T.; Hao, L.; Wei, Y.; Cai, X.; Zhu, B. Doxorubicin conjugated carbon dots as a drug delivery system for human breast cancer therapy. *Cell Prolif.* **2018**, *51*, e12488. [[CrossRef](#)]
65. Wen, Z.; Yin, X. Excitation-independent carbon dots, from photoluminescence mechanism to single-color application. *RSC Adv.* **2016**, *6*, 27829. [[CrossRef](#)]

66. Reckmeier, C.J.; Schneider, J.; Xiong, Y.; Häusler, J.; Kasák, P.; Schnick, W.; Rogach, A.L. Aggregated molecular fluorophores in the ammonothermal synthesis of carbon dots. *Chem. Mater.* **2017**, *29*, 10352. [[CrossRef](#)]
67. Sharma, A.; Gady, T.; Gupta, A.; Ballal, A.; Ghosh, S.K.; Kumbhakar, M. Origin of excitation dependent fluorescence in carbon nanodots. *J. Phys. Chem. Lett.* **2016**, *7*, 3695. [[CrossRef](#)]
68. Sun, C.; Zhang, Y.; Sun, K.; Reckmeier, C.; Zhang, T.; Zhang, X.; Zhao, J.; Wu, C.; William, W.Y.; Rogach, A.L. Combination of carbon dot and polymer dot phosphors for white light-emitting diodes. *Nanoscale* **2015**, *7*, 12045. [[CrossRef](#)]
69. Wu, Z.L.; Gao, M.X.; Wang, T.T.; Wan, X.Y.; Zheng, L.L.; Huang, C.Z. A general quantitative pH sensor developed with dicyandiamide N-doped high quantum yield graphene quantum dots. *Nanoscale* **2014**, *6*, 3868. [[CrossRef](#)]
70. Zuo, P.; Liu, J.; Guo, H.; Wang, C.; Liu, H.; Zhang, Z.; Liu, Q. Multifunctional N, S co-doped carbon dots for sensitive probing of temperature, ferric ion, and methotrexate. *Anal. Bioanal. Chem.* **2019**, *411*, 1647. [[CrossRef](#)]
71. Liu, Y.; Zhou, L.; Li, Y.; Deng, R.; Zhang, H. Highly fluorescent nitrogen-doped carbon dots with excellent thermal and photo stability applied as invisible ink for loading important information and anti-counterfeiting. *Nanoscale* **2017**, *9*, 491. [[CrossRef](#)] [[PubMed](#)]
72. Wang, H.; Lu, Q.; Hou, Y.; Liu, Y.; Zhang, Y. High fluorescence S, N co-doped carbon dots as an ultra-sensitive fluorescent probe for the determination of uric acid. *Talanta* **2016**, *155*, 62. [[CrossRef](#)] [[PubMed](#)]
73. Schneider, J.; Reckmeier, C.J.; Xiong, Y.; Von Seckendorff, M.; Susha, A.S.; Kasák, P.; Rogach, A.L. Molecular fluorescence in citric acid-based carbon dots. *J. Phys. Chem.* **2017**, *121*, 2014. [[CrossRef](#)]
74. Zhang, Y.; Liu, X.; Fan, Y.; Guo, X.; Zhou, L.; Lv, Y.; Lin, J. One-step microwave synthesis of N-doped hydroxyl-functionalized carbon dots with ultra-high fluorescence quantum yields. *Nanoscale* **2016**, *8*, 15281. [[CrossRef](#)]
75. Ding, H.; Wei, J.; Zhong, N.; Gao, Q.; Xiong, H. Highly efficient red-emitting carbon dots with gram-scale yield for bioimaging. *Langmuir* **2017**, *33*, 12635. [[CrossRef](#)]
76. Li, D.; Jing, P.; Sun, L.; An, Y.; Shan, X.; Lu, X.; Zhou, D.; Han, D.; Shen, D.; Zhai, Y. Near-infrared excitation/emission and multiphoton-induced fluorescence of carbon dots. *Adv. Mater.* **2018**, *30*, 1705913. [[CrossRef](#)]
77. Anjana, R.; Devi, J.A.; Jayasree, M.; Aparna, R.; Aswathy, B.; Praveen, G.; Lekha, G.; Sony, G. S, N-doped carbon dots as a fluorescent probe for bilirubin. *Microchim. Acta* **2018**, *185*, 11. [[CrossRef](#)]
78. Zhang, W.; Shi, L.; Liu, Y.; Meng, X.; Xu, H.; Xu, Y.; Liu, B.; Fang, X.; Li, H.; Ding, T. Supramolecular interactions via hydrogen bonding contributing to citric-acid derived carbon dots with high quantum yield and sensitive photoluminescence. *RSC Adv.* **2017**, *7*, 20345. [[CrossRef](#)]
79. Liu, Q.; Zhang, N.; Shi, H.; Ji, W.; Guo, X.; Yuan, W.; Hu, Q. One-step microwave synthesis of carbon dots for highly sensitive and selective detection of copper ions in aqueous solution. *New J. Chem.* **2018**, *42*, 3097. [[CrossRef](#)]
80. Hou, J.; Wang, W.; Zhou, T.; Wang, B.; Li, H.; Ding, L. Synthesis and formation mechanistic investigation of nitrogen-doped carbon dots with high quantum yields and yellowish-green fluorescence. *Nanoscale* **2016**, *8*, 11185. [[CrossRef](#)]
81. Cheng, J.; Wang, C.; Zhang, Y.; Yang, S.; Chen, S. Zinc ion-doped carbon dots with strong yellow photoluminescence. *RSC Adv.* **2016**, *6*, 37189. [[CrossRef](#)]
82. Zhu, Z.; Cheng, R.; Ling, L.; Li, Q.; Chen, S. Rapid and large-scale production of multi-fluorescence carbon dots via magnetic hyperthermia method. *Angew. Chem. Int. Ed.* **2019**, *59*, 3099. [[CrossRef](#)] [[PubMed](#)]
83. Li, H.; Ye, S.; Guo, J.; Kong, J.; Song, J.; Kang, Z. The design of room-temperature-phosphorescent carbon dots and their application as a security ink. *J. Mater. Chem.* **2019**, *7*, 10605. [[CrossRef](#)]
84. Xie, Z.; Zheng, M. Colour-tunable ultralong-lifetime room temperature phosphorescence with external heavy-atom effect in boron-doped carbon dots. *Chem. Eng. J.* **2020**, 127647. [[CrossRef](#)]
85. Liu, E.; Li, D.; Zhou, X.; Zhou, G.; Xiao, H.; Zhou, D.; Tian, P.; Guo, R.; Qu, S. Highly emissive carbon dots in solid state and their applications in light-emitting devices and visible light communication. *ACS Sustain. Chem. Eng.* **2019**, *7*, 9301. [[CrossRef](#)]
86. Kalytchuk, S.; Poláková, K.I.; Wang, Y.; Froning, J.P.; Cepe, K.; Rogach, A.L.; Zbořil, R. Carbon dot nanothermometry: Intracellular photoluminescence lifetime thermal sensing. *ACS Nano* **2017**, *11*, 1432. [[CrossRef](#)]
87. Mohammed, L.J.; Omer, K.M. Carbon dots as new generation materials for nanothermometer. *Nanoscale Res. Lett.* **2020**, *15*, 182. [[CrossRef](#)]
88. Meierhofer, F.; Dissinger, F.; Weigert, F.; Jungclaus, J.; Müller-Caspary, K.; Waldvogel, S.R.; Resch-Genger, U.; Voss, T. Citric acid based carbon dots with amine type stabilizers: pH-specific luminescence and quantum yield characteristics. *J. Phys. Chem.* **2020**, *124*, 8894. [[CrossRef](#)]
89. Stagi, L.; Mura, S.; Malfatti, L.; Carbonaro, C.M.; Ricci, P.C.; Porcu, S.; Secci, F.; Innocenzi, P. Anomalous optical properties of citrazinic acid under extreme pH conditions. *ACS Omega* **2020**. [[CrossRef](#)]
90. Mura, S.; Stagi, L.; Ludmerczki, R.; Malfatti, L.; Innocenzi, P. Reversible aggregation of molecular-like fluorophores driven by extreme pH in carbon dots. *Materials* **2020**, *13*, 3654. [[CrossRef](#)]
91. Mura, S.; Stagi, L.; Malfatti, L.; Carbonaro, C.M.; Ludmerczki, R.; Innocenzi, P. Modulating the optical properties of citrazinic acid through the monomer-to-dimer transformation. *J. Phys. Chem.* **2019**, *124*, 197. [[CrossRef](#)] [[PubMed](#)]
92. Xie, Z.; Du, Q.; Wu, Y.; Hao, X.; Liu, C. Full-band UV shielding and highly daylight luminescent silane-functionalized graphene quantum dot nanofluids and their arbitrary polymerized hybrid gel glasses. *J. Mater. Chem.* **2016**, *4*, 9879. [[CrossRef](#)]
93. Wang, H.; Sun, P.; Cong, S.; Wu, J.; Gao, L.; Wang, Y.; Dai, X.; Yi, Q.; Zou, G. Nitrogen-doped carbon dots for “green” quantum dot solar cells. *Nanoscale Res. Lett.* **2016**, *11*, 27. [[CrossRef](#)] [[PubMed](#)]

94. Zhang, Y.; Park, M.; Kim, H.Y.; Ding, B.; Park, S.-J. A facile ultrasonic-assisted fabrication of nitrogen-doped carbon dots/BiOBr up-conversion nanocomposites for visible light photocatalytic enhancements. *Sci. Rep.* **2017**, *7*, 45086. [[CrossRef](#)] [[PubMed](#)]
95. Liu, J.; Ren, J.; Xie, Z.; Guan, B.; Wang, J.; Ikeda, T.; Jiang, L. Multi-functional organosilane-polymerized carbon dot inverse opals. *Nanoscale* **2018**, *10*, 4642. [[CrossRef](#)]
96. Liu, J.; Xie, Z.; Shang, Y.; Ren, J.; Hu, R.; Guan, B.; Wang, J.; Ikeda, T.; Jiang, L. Lyophilic but nonwetttable organosilane-polymerized carbon dots inverse opals with closed-cell structure. *ACS Appl. Mater. Interfaces* **2018**, *10*, 6701. [[CrossRef](#)]
97. Zhang, W.; Ni, Y.; Xu, X.; Lu, W.; Ren, P.; Yan, P.; Siu, C.K.; Ruan, S.; Yu, S.F. Realization of multiphoton lasing from carbon nanodot microcavities. *Nanoscale* **2017**, *9*, 5957. [[CrossRef](#)]
98. Shangguan, J.; He, D.; He, X.; Wang, K.; Xu, F.; Liu, J.; Tang, J.; Yang, X.; Huang, J. Label-free carbon-dots-based ratiometric fluorescence pH nanoprobes for intracellular pH sensing. *Anal. Chem.* **2016**, *88*, 7837. [[CrossRef](#)]
99. Chen, Y.; Sun, X.; Wang, X.; Pan, W.; Yu, G.; Wang, J. Carbon dots with red emission for bioimaging of fungal cells and detecting Hg<sup>2+</sup> and ziram in aqueous solution. *Spectrochim. Acta Part A Mol. Biomol. Spectrosc.* **2020**, 118230. [[CrossRef](#)]
100. Wang, X.; Yan, P.; Kerns, P.; Suib, S.L.; Loew, L.; Zhao, J. Voltage-dependent photoluminescence of carbon dots. *J. Electrochem. Soc.* **2020**, *167*, 147515. [[CrossRef](#)]
101. Zeng, Q.; Shao, D.; He, X.; Ren, Z.; Ji, W.; Shan, C.; Qu, S.; Li, J.; Chen, L.; Li, Q. Carbon dots as a trackable drug delivery carrier for localized cancer therapy in vivo. *J. Mater. Chem.* **2016**, *4*, 5119. [[CrossRef](#)] [[PubMed](#)]
102. Ji, Z.; Yin, Z.; Jia, Z.; Wei, J. Carbon nanodots derived from urea and citric acid in living cells: Cellular uptake and antioxidation effect. *Langmuir* **2020**, *36*, 8632. [[CrossRef](#)] [[PubMed](#)]
103. Wang, H.; Zhang, M.; Ma, Y.; Wang, B.; Huang, H.; Liu, Y.; Shao, M.; Kang, Z. Carbon dots derived from citric acid and glutathione as a highly efficient intracellular reactive oxygen species scavenger for alleviating the lipopolysaccharide-induced inflammation in macrophages. *ACS Appl. Mater. Interfaces* **2020**, *12*, 41088. [[CrossRef](#)] [[PubMed](#)]
104. Liu, H.; Li, Z.; Sun, Y.; Geng, X.; Hu, Y.; Meng, H.; Ge, J.; Qu, L. Synthesis of luminescent carbon dots with ultrahigh quantum yield and inherent folate receptor-positive cancer cell targetability. *Sci. Rep.* **2018**, *8*, 1086. [[CrossRef](#)] [[PubMed](#)]
105. Zhang, T.; Zhu, J.; Zhai, Y.; Wang, H.; Bai, X.; Dong, B.; Wang, H.; Song, H. A novel mechanism for red emission carbon dots: Hydrogen bond dominated molecular states emission. *Nanoscale* **2017**, *9*, 13042. [[CrossRef](#)] [[PubMed](#)]
106. Ding, H.; Wei, J.S.; Zhang, P.; Zhou, Z.Y.; Gao, Q.Y.; Xiong, H.M. Solvent-controlled synthesis of highly luminescent carbon dots with a wide color gamut and narrowed emission peak widths. *Small* **2018**, *14*, 1800612. [[CrossRef](#)]